

# Quantum size effects in the nonmetal to metal transition of two-dimensional Al islands

Ying Jiang,<sup>1,2</sup> Kehui Wu,<sup>1</sup> Jie Ma,<sup>1</sup> Biao Wu,<sup>1</sup> E. G. Wang,<sup>1</sup> and Ph. Ebert<sup>2</sup>

<sup>1</sup>*Institute of Physics, Chinese Academy of Sciences, Beijing 100080, China*

<sup>2</sup>*Institut für Festkörperforschung, Forschungszentrum Jülich GmbH, 52425 Jülich, Germany*

(Received 12 October 2007; published 27 December 2007)

Nonmetal-metal transitions are generally described by models which correlate the electronic transitions to structural changes. Here, we present a semiconductor-metal transition without structural changes. By combining scanning tunneling microscopy and high-resolution electron energy loss spectroscopy, we found that the band gap of two-dimensional (2D) Al islands grown on Si(111)- $\sqrt{3} \times \sqrt{3}$ -Al substrates decreases with increasing island size. We argue that this purely size dependent effect arises from the lateral confinement of free electrons in a 2D potential well formed by the islands.

DOI: [10.1103/PhysRevB.76.235434](https://doi.org/10.1103/PhysRevB.76.235434)

PACS number(s): 73.22.-f, 68.37.Ef, 71.30.+h

## I. INTRODUCTION

The ability to reproducibly engineer band gaps at surfaces is essential for various technological applications of surface-based system, e.g., as sensors or catalysts. One possibility of modifying the band gap is to utilize a nonmetal-metal transition at semiconductor surfaces. Thin films of materials, normally considered to be metals, may possess nonmetallic properties at submonolayer coverages on semiconducting substrates. With increasing deposition amount, these films experience, however, a nonmetal-metal transition. There are several different physical models to describe this transition in two-dimensional metal systems, generally classified into the Wilson, Peierls or charge density wave, and Mott-Hubbard transitions.<sup>1</sup> Despite clear differences, all these models connect the nonmetal-metal transition to structural changes in the metallic overlayer, such as, e.g., transitions between one-, two-, and/or three-dimensional growth,<sup>2</sup> lattice expansions or contractions,<sup>3</sup> or the formation of electronic or atomic superstructures.<sup>4</sup> At present, there is no example of a nonmetal-metal transition without structural changes of the metallic overlayer.<sup>5</sup> In this paper, we show, however, that two-dimensional (2D) monatomic high Al islands grown on Si(111)- $\sqrt{3} \times \sqrt{3}$ -Al substrates exhibit a continuous band gap reduction leading to a semiconductor-metal transition with increasing island size, despite the islands keeping their atomic structure unchanged. We argue that the lateral *spatial* confinement of electrons in the islands, i.e., the so-called quantum size effect, induces the change of the band gap and, thereby, the semiconductor-metal transition without any need of structural changes of the island's atomic structure.

## II. EXPERIMENT

We illustrate this effect by combining the spatial information about the island's size and structure obtained by scanning tunneling microscopy (STM) and the electronic properties, i.e., the size of the gap, derived from high-resolution electron energy loss spectroscopy (HREELS). The experiments were carried out in a combined VT-STM (Omicron) and HREELS (LK-5000) ultrahigh vacuum system ( $p < 1 \times 10^{-10}$  mbar). Si samples (*n* type, resistivity of  $2 \Omega \text{ cm}$ ) were cleaned by flashing above  $1000^\circ \text{C}$  followed by a slow

cool down to room temperature. This yielded well-ordered Si(111)- $7 \times 7$  surfaces, on which 0.16 ML Al [rate of 0.07 ML/min in terms of the atomic density of the Al(111) plane] were deposited at room temperature followed by annealing to  $720^\circ \text{C}$  for 2 min. The resulting Si(111)- $\sqrt{3} \times \sqrt{3}$ -Al surface was used as substrate for the subsequent growth of Al islands at 100 K. After warm up to room temperature, the sample was investigated *in situ* by STM and HREELS. For the HREELS measurement, we used the specular scattering geometry with an incident electron energy of 50 eV and an incident angle of  $55^\circ$  with respect to the surface normal.

## III. RESULTS AND DISCUSSIONS

Figure 1 illustrates the initial stages of Al growth on Si(111)- $\sqrt{3} \times \sqrt{3}$ -Al substrates. 2D islands with a height of 0.2 nm (single monolayer height) form. With increasing coverage, the height of the islands does not change, but their lateral size becomes larger. The increase of the lateral size is corroborated by the corresponding size distributions of the Al islands [Figs. 1(a2)–1(c2)]. At coverages  $> 0.58$  ML, the 2D islands percolate [Fig. 2(c)]. The particularity of this system is the growth of 2D monolayer high metal islands on a semiconductor surface.

The atomic structure of the islands can be derived using high-resolution STM images, such as the one shown in Fig. 2(a). The STM image shows the  $\sqrt{3} \times \sqrt{3}$  structure of the uncovered substrate and islands exhibiting a hexagonal moiré pattern with a periodicity length of  $1.15 \pm 0.10$  nm (see indicated unit cell). Corresponding low energy electron diffraction (LEED) patterns [Fig. 2(b)] show three types of spots assignable to the Si(111) $\sqrt{3} \times \sqrt{3}$ , Si(111) $1 \times 1$ , and Al(111) $1 \times 1$  structures. The  $\sqrt{3} \times \sqrt{3}$  spots become increasingly fainter with increasing coverage, and disappear eventually at full coverage of 1 ML. This suggests that the islands consist of an Al(111) $1 \times 1$  structure directly on top of a Si(111) $1 \times 1$  substrate, replacing the  $\sqrt{3} \times \sqrt{3}$  structure.<sup>6</sup> This is corroborated by the periodicity length ( $a_{\text{moiré}}$ ) of the moiré pattern, which is consistent with the relative lattice constants of Si(111) $1 \times 1$  and Al(111) $1 \times 1$ , i.e.,  $3a_{\text{Si}} = 4a_{\text{Al}} = a_{\text{moiré}}$ . Furthermore, detailed coverage measurements for the complete layer also support this structure.<sup>6</sup>

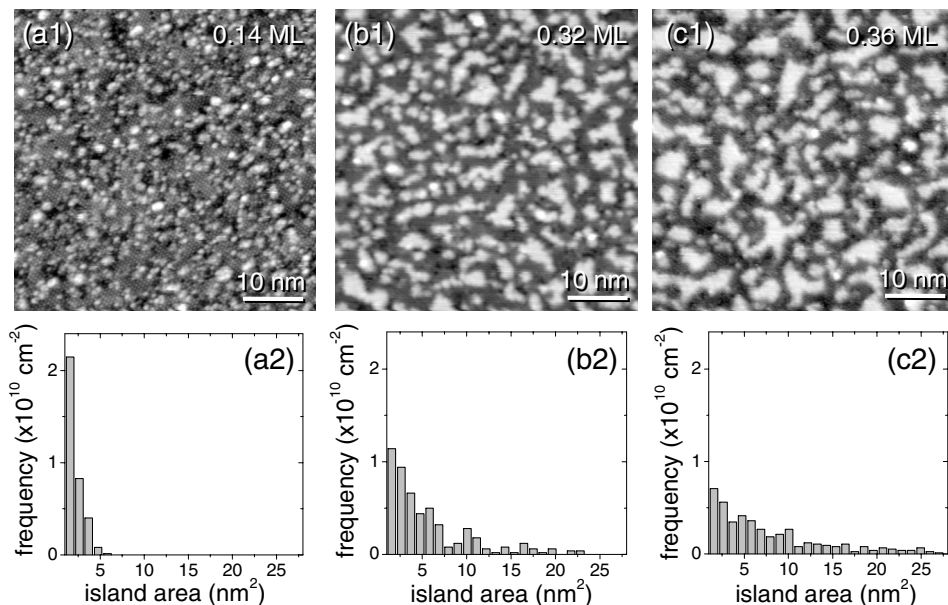


FIG. 1. [(a1)–(c1)] Empty state constant-current STM images of the evolution of Al islands grown on Si(111)- $\sqrt{3} \times \sqrt{3}$ -Al substrates with increasing Al coverage. (a2)–(c2) show the corresponding island size distributions.

At this stage, we turn to the structure of the islands as a function of their size. While individual Al atoms in the islands could not be directly imaged due to the weak corrugation, we can investigate the size dependence of the structure using the moiré patterns and height measurements. Figure 2(d) shows the dependence of the periodicity length of the moiré pattern (filled squares) and of the island height (empty symbols) as a function of the area of the islands. Both properties remain constant down to island sizes of 2.5 nm<sup>2</sup>. Only

below 2.5 nm<sup>2</sup> size, the islands have a lower height, suggesting that their structure is different. Indeed, such small islands appear rather as clusters. For larger islands, however, the high sensitivity of the moiré patterns on small changes in the lattice parameters indicates that the structure of the islands remains essentially unchanged. Note that islands below about 8 nm<sup>2</sup> do not exhibit visible moiré patterns, since the size of the island is too small compared to the unit cell of the moiré pattern. Nevertheless, the unchanged height down to

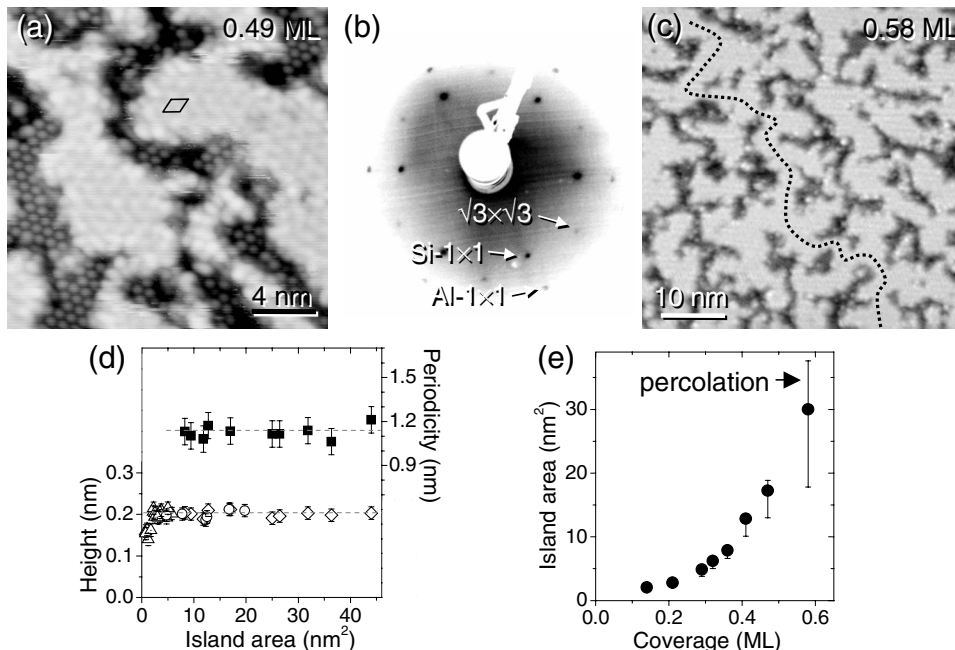


FIG. 2. High-resolution empty state (a) STM image and (b) corresponding LEED pattern of Al islands on the Si(111)- $\sqrt{3} \times \sqrt{3}$ -Al substrate (coverage of 0.49 ML Al). The islands exhibit a moiré pattern (see marked unit cell). (c) Percolating island structures at 0.58 ML coverage. The dashed line indicates the percolation. (d) Periodicity length of the moiré pattern (right scale) and height of the islands relative to the Si(111)- $\sqrt{3} \times \sqrt{3}$ -Al substrate (left scale) as a function of the island size (measured at  $2 \pm 0.1$  V sample voltage). The data suggest that the islands larger than 2.5 nm<sup>2</sup> have identical Al(111)  $1 \times 1$  structures. (e) Average island size as a function of the Al coverage. The large error bar of the uppermost data point is due to percolated islands present above about 0.58 ML coverage.

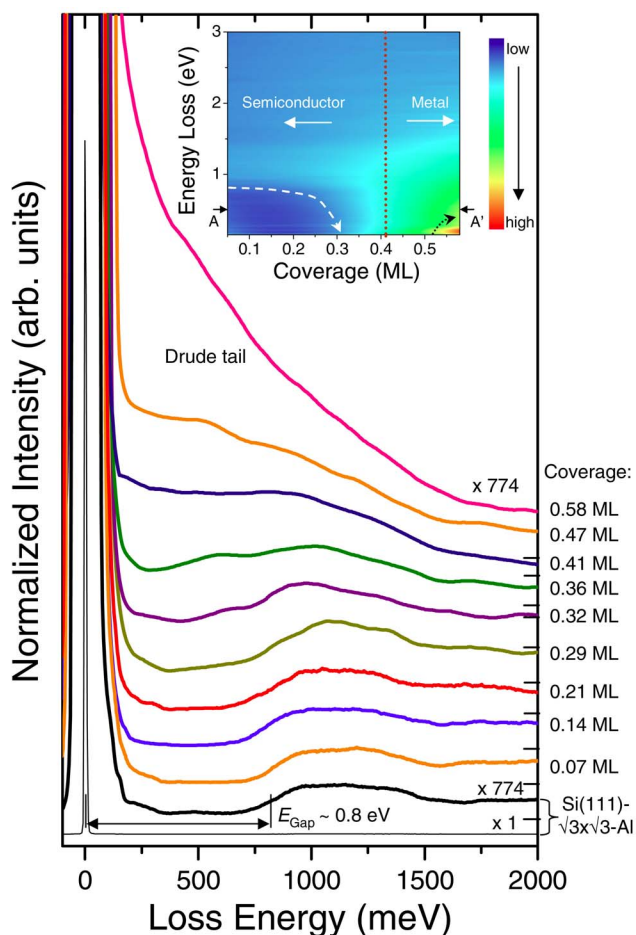


FIG. 3. (Color online) Al coverage dependence of electron energy loss spectra. All spectra are normalized by the intensity of the elastic peak. The individual spectra are vertically offset. The respective zero intensities are indicated by small dashes on the right scale. With increasing deposition amount, the band gap of initially about 0.8 eV decreases and, at high coverages, a metallic Drude tail appears. Inset: 2D intensity map of the EELS data. The narrowing of the band gap is indicated by the white arrow. The effect of percolation in the EELS data is indicated by the black arrow.

sizes of about  $2.5 \text{ nm}^2$  suggests, even here, the presence of the same Al(111) $1 \times 1$  atomic arrangement. Thus, we focus here only on the islands larger than  $2.5 \text{ nm}^2$  with identical atomic structure.

In order to correlate the size of the islands with their electronic properties, we measured corresponding electron energy loss spectroscopy (EELS) spectra for every Al coverage investigated by STM (Fig. 3). The spectrum obtained on the clean Si(111)- $\sqrt{3} \times \sqrt{3}$ -Al substrate (black spectra at the bottom of Fig. 3) shows around 0 eV energy loss the elastic peak, which is of no further interest here, and up to about 0.8 eV a low intensity arising from the presence of an electronic band gap, where no states can be excited. The presence of a band gap has also been found by scanning tunneling spectroscopy<sup>7</sup> (STS) and predicted theoretically.<sup>8</sup> The size of the band gap measured here arises from excitations of both surface states and near surface Si bulk states. Upon

increasing deposition of Al, the gap gradually narrows until a metallic loss continuum (Drude tail) appears and fills the gap at 0.58 ML.<sup>9</sup> This indicates that with increasing coverage, a semiconductor-metal transition occurs.

For illustration purposes, we convert the series of the EELS data into a 2D energy loss vs coverage intensity map using the Shepard gridding method (inset in Fig. 3). The band gap is visible in the 2D intensity plot as a dark blue zone in the lower left corner. The band gap narrows from the high energy loss side, as indicated by the bended white dashed arrow and further corroborated by the quantitative discussion below. In addition, the EELS intensity cannot be simply described as the area weighted sum of the substrate and a metallic overlayer. Thus, the gap narrowing cannot be the result of an accumulating Drude tail intensity with increasing coverage, something which occurs in a percolated island system. Indeed, above 0.58 ML, STM images show the formation of percolated island structures [Fig. 2(c)], which are coupled to a sudden increase of the EELS intensity in the lower right corner of the 2D intensity map (curved black dotted arrow). This indicates that at the transition from isolated to percolated islands the resistivity of the Al film decreases, an effect found previously for Ag films on Si(111) $7 \times 7$  substrates.<sup>10</sup> Here, we focus, however, on the band gap narrowing leading to the semiconductor-metal transition of isolated islands before the percolation onset.

From the EELS data, we extract the band gap vs coverage, which is schematically indicated by the bended dashed white arrow (inset in Fig. 3). A quantitative extraction of the band gap can be done by identifying the intensity increase with increasing loss energy for a *fixed coverage* (vertical cut in the 2D intensity map). Due to the small differences in intensity, this method is, however, inaccurate. Therefore, we extracted horizontal cuts of the EELS intensity vs coverage at different *fixed chosen loss energies* (example cut marked A-A'). Such intensity cuts are shown in the inset of Fig. 4(a) for different loss energies. They exhibit threshold coverages, where the rate of increase of the EELS intensity changes. This change at the threshold coverage arises from the onset of additional valence to conduction band excitations,<sup>11</sup> giving rise to the specific loss energy chosen. Thus, at a particular threshold coverage, the band gap of the surface system is equal to the loss energy chosen and, therefore, the band gap vs coverage relation is given by the loss energy vs the threshold coverage.

The thus obtained band gap vs coverage can be transformed into a band gap vs island size relation [filled circles in Fig. 4(a)] using the average island size vs coverage derived from the STM images [Fig. 2(e)]. The average island sizes are derived from island size distributions as those shown in Fig. 1. The determination of an island size by STM inherently gives rise to systematic errors due to tip-convolution effects. Unfortunately, the tip state and radius are never known during an experiment. We, however, used only images which showed every individual atom on the Si(111)- $\sqrt{3} \times \sqrt{3}$ -Al substrate on which the islands were grown. In order to estimate the maximum errors possible, we used a tip radius of 2 nm, where all atomic resolution would be removed by convolution. Then, the systematic error bars lower the lower side error bar only. The sum of the statistical

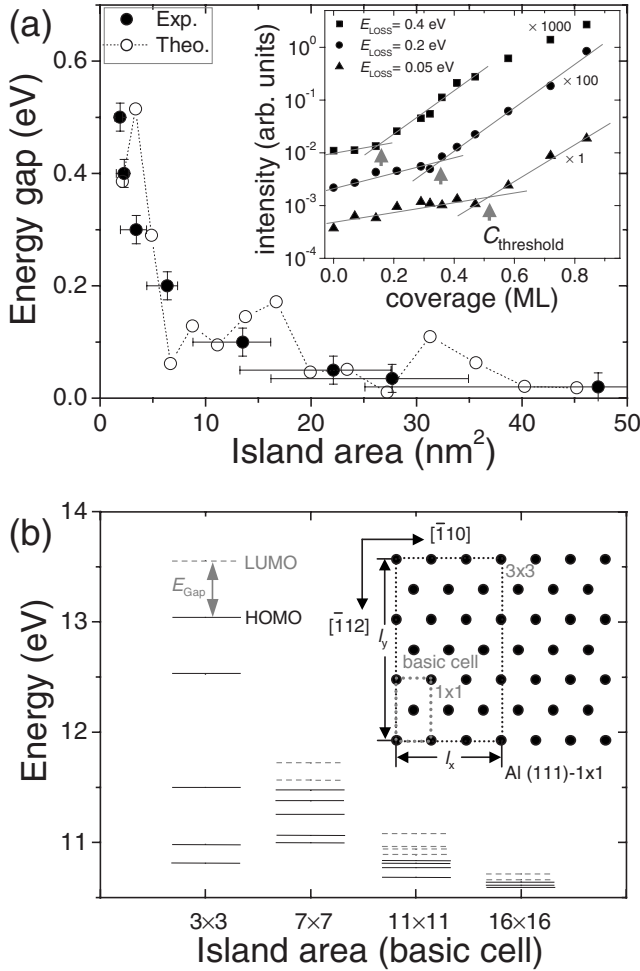


FIG. 4. (a) Band gap vs the average area of the islands. Experimental and calculated data points are shown as filled and open circles, respectively. Inset: Electron energy loss intensity at three fixed loss energies as a function of the coverage. The respective threshold coverages are indicated by the arrows. The extracted energy-threshold coverage pairs are used to derive the functional dependence of the band gap on the island size shown in (a) with help of Fig. 2(d) (see text). (b) Calculated energy levels for several rectangular Al islands with different sizes in the vicinity of the Fermi energy. The band gap is the difference between the highest occupied (labeled HOMO) and lowest unoccupied (LUMO) energy level. Filled and empty energy levels are shown as solid black and dashed gray lines, respectively. The inset shows the selected island geometries used for the calculation of the energy levels.

errors, given by the standard deviation of different images, and the maximum systematic ones are shown in Fig. 2(e) and used for further analysis. However, noting that the much higher resolution of the images and the fact that the island size is not measured at the bottom of the step, but at the top, where convolution effects of the tip are negligible, we expect that the systematic error to be *much smaller* than shown, such that the lower error bar approaches the size of the upper one.

The resulting band gap vs island size relation [filled circles in Fig. 4(a)] shows a clear decrease of the band gap with increasing island size. The large band gaps at small

island sizes clearly indicate semiconducting properties, while the small to vanishing band gaps at large island sizes demonstrate a gradual change to metallic properties. The gradual change makes the determination of the exact point of a semiconductor-metal transition somewhat difficult. However, the semiconductor-metal transition can be identified using the criterium  $E_{\text{gap}} \approx 3kT$  at the transition, as defined and discussed in Ref. 1. On this basis, the transition occurs at island sizes of 15–20 nm<sup>2</sup>, without structural transition in the islands.

Furthermore, the point of a semiconductor-metal transition can also be defined by the conductivity. The conductivity is, however, closely related to the band gap. Since we do not have any information about the conductivity, we used the criterium  $E_{\text{gap}} \approx 3kT$  to define the transition point in our continuous change of the band gap with island size. Other criteria may yield slightly different island sizes for the transition point, but the essential physics, i.e., that the band gap is reduced continuously down to zero and that there is, as a consequence, a semiconductor-metal transition with increasing island size with no structural changes, remains unchanged.

All models outlined above are based on structural changes. Hence, they cannot be applied to describe our observed semiconductor-metal transition. Thus, we turn to a model which only involves the size of the islands, i.e., the lateral confinement of electrons in 2D islands. Since Al is a metal with nearly free electrons, we model the islands as a noninteracting electron gas confined in a 2D potential well with infinite barriers. Despite its simplicity, this model allows us to capture the essence of the physics involved.

The energies of an electron in a rectangular potential well of width  $l_x$  and length  $l_y$  [see inset of Fig. 4(b)] are given by  $E_{n_x, n_y} = (\pi^2 \hbar^2 / 2m) [(n_x^2 / l_x^2) + (n_y^2 / l_y^2)]$ , where  $m$  is the free electron mass, and  $n_x$  and  $n_y$  are the quantum numbers. The resulting discrete energy levels near the Fermi energy are shown in Fig. 4(b) for several 2D potential wells with different lateral dimensions  $i \times j$  of a rectangular chosen  $1 \times 1$  basic cell. It is evident that the separation between the energy levels is increasing with decreasing lateral size of the island. In order to identify the size of the electronic band gap, we filled the energy levels with electrons up to charge neutrality. The energy difference between the highest occupied and the lowest unoccupied levels (labeled HOMO and LUMO, respectively) corresponds to the band gap. In addition, we took into account a possible phase shift of the electron waves at the boundaries of the islands.<sup>12</sup> Such a phase shift is equivalent to a change by  $2 \times \Delta l$  of the dimensions of the potential well.<sup>13</sup> Thus, the effective island size is given by  $l_x - 2 \times \Delta l$  and  $l_y - 2 \times \Delta l$ , where  $l_x$  and  $l_y$  are the dimensions of a potential well with no phase shift.

The calculated band gaps are shown as empty circles in Fig. 4(a), with  $\Delta l$  as the only fitting parameter. The calculated band gaps reproduce the experimental observations well. We also calculated the band gaps for islands with different aspect ratios (i.e., 1/1, 2/1, 3/1, and 3/2). The values all remain inside the range given by the fluctuations of the band gaps of the quadratic islands. Thus, the band gap vs size values obtained for quadratic islands is representative of different island shapes. The fluctuations of the calculated val-

ues cannot be observed in the experimental values, since EELS measurements average the excitations of all island shapes and sizes present on the surface, while the calculated values refer to specific island geometries. This averaging effect might smear out the details of the gap variation, but the overall trend remains unaffected. The agreement indicates that quantum size effects determine the band gap of our Al islands and, thus, govern the semiconductor-metal transition.

The best fit is obtained with a phase shift of  $\Delta l = -0.4 \pm 0.2$  nm, i.e., the potential well dimensions are *reduced* compared to the island size. Phase shifts are typically ascribed to charge spillages at the confining boundaries<sup>12,13</sup> and can be estimated using Eq. (24) of Ref. 13 to about  $+0.07$  nm in our case. This value is significantly smaller than the measured one and it would increase, not reduce, the effective size of the potential. This suggests additional factors affecting the phase shift. Indeed, high-resolution STM images [see Fig. 2(a)] show that the islands exhibit a slightly disordered edge, which is consistent with the observed reduced effective size of the potential well.

We emphasize that the change of the band gap is continuous, unlike in the cases of other semiconductor-metal transitions where structural changes induce sudden jumps in the electronic properties. Thus, the fact that we observe a continuous change of the band gap supports our conclusion that no structural effects dominate the band gap, except for quantum size effects. Furthermore, a continuous change of the band gap induces a semiconductor-metal transition as well as sudden structural changes. The mere fact that the exact transition point is more difficult to define due to the continuity does not change the fact that with increasing island size, the band gap is reduced to zero and, thus, a normal metallic band structure is reached. Therefore, our system can be considered as a semiconductor-metal transition.

Finally, in principle, one could detect the size of the band gap of individual islands with no averaging effect by STS.

However, on unpinned semiconductor surfaces, such as ours, the apparent size of the band gap in tunneling spectra is almost always larger than the real one, and highly sensitive to the dopant level and type.<sup>14</sup> This is due to tip-induced band bending effects, which hamper the extraction of the real band gap at low dopant levels,<sup>14,15</sup> as in our case. EELS is, however, not affected by this and, thus, provides the real gap as long as it is smaller than the onset of the band to band excitations of the substrate.

#### IV. CONCLUSIONS

By combining STM and HREELS measurements, we observed a semiconductor-metal transition in 2D monolayer high Al islands grown on Si(111)- $\sqrt{3} \times \sqrt{3}$ -Al substrates. The band gap of the islands is found to decrease with increasing size of the islands, although no changes in the structure of the Al(111)  $1 \times 1$  islands occur. We argue that this purely size dependent semiconductor-metal transition arises from the lateral confinement of free electrons in a 2D potential well formed by the islands. Thus, not only structural transitions in the metallic overlayer can induce nonmetal-metal transitions as demonstrated numerous times before, but also quantum size effects. Furthermore, this example illustrates the possibility to precisely engineer the desired average band gap at semiconductor surfaces using this peculiar growth of 2D metal islands on silicon.

#### ACKNOWLEDGMENTS

The authors acknowledge financial support from the National Natural Science Foundation, the MOST of China, and the CAS, as well as partial financial support from the Deutsche Forschungsgemeinschaft.

<sup>1</sup>P. A. Dowben, Surf. Sci. Rep. **40**, 151 (2000), and references therein. In addition to the mentioned types of transition, there are further ones which, however, cannot be applied successfully to thin metal films grown on semiconductor substrates.

<sup>2</sup>N. J. DiNardo, T. M. Wong, and E. W. Plummer, Phys. Rev. Lett. **65**, 2177 (1990); L. J. Whitman, J. A. Stroscio, R. A. Dragoset, and R. J. Celotta, *ibid.* **66**, 1338 (1991).

<sup>3</sup>J.-H. Cho, Q. Niu, and Z. Y. Zhang, Phys. Rev. Lett. **80**, 3582 (1998).

<sup>4</sup>S. J. Park, H. W. Yeom, S. H. Min, D. H. Park, and I.-W. Lyo, Phys. Rev. Lett. **93**, 106402 (2004); R. Cortés, A. Tejada, J. Lobo, C. Didiot, B. Kierren, D. Malterre, E. G. Michel, and A. Mascaraque, *ibid.* **96**, 126103 (2006).

<sup>5</sup>Nonmetal-metal transitions with increasing feature size were observed previously, but no structural information is available. See, e.g., J. D. Zhang, D. Q. Li, and P. W. Dowben, J. Phys.: Condens. Matter **6**, 33 (1994); P. N. First, J. A. Stroscio, R. A. Dragoset, D. T. Pierce, and R. J. Celotta, Phys. Rev. Lett. **63**, 1416 (1989); R. Busani, M. Folkers, and O. Cheshnovsky, *ibid.* **81**, 3836 (1998); O. C. Thomas, W. Zheng, S. Xu, and K. H. Bowen, Jr., *ibid.* **89**, 213403 (2002).

<sup>6</sup>Y. Jiang, K. H. Wu, Z. Tang, Ph. Ebert, and E. G. Wang, Phys. Rev. B **76**, 035409 (2007).

<sup>7</sup>R. J. Hamers, Phys. Rev. B **40**, 1657 (1989).

<sup>8</sup>J. E. Northrup, Phys. Rev. Lett. **53**, 683 (1984).

<sup>9</sup>H. Ibach and D. L. Mills, *Electron Energy Loss Spectroscopy and Surface Vibrations* (Academic, New York, 1982).

<sup>10</sup>L. Gavioli, K. R. Kimberlin, M. C. Tringides, J. F. Wendelken, and Z. Zhang, Phys. Rev. Lett. **82**, 129 (1999).

<sup>11</sup>The slow increase of the EELS intensity below the threshold coverage is due to the increasing coverage, raising the statistical presence of a very small fraction of large metallic islands. The overall EELS signal is, however, still dominated by the average sized islands.

<sup>12</sup>T. C. Chiang, Surf. Sci. Rep. **39**, 181 (2000).

<sup>13</sup>P. Czoschke, H. Hong, L. Basile, and T.-C. Chiang, Phys. Rev. B **72**, 075402 (2005).

<sup>14</sup>N. D. Jäger, E. R. Weber, K. Urban, and Ph. Ebert, Phys. Rev. B **67**, 165327 (2003).

<sup>15</sup>N. D. Jäger, M. Marco, E. R. Weber, K. Urban, and P. Ebert, Phys. Rev. B **67**, 165307 (2003).